

Magnetic Properties of $\text{La}_{0.8}\text{K}_{0.2}\text{MnO}_3$ Nanoparticles

M. MIHALIK^{a,*}, M. ZENTKOVÁ^a, J. BRIANČIN^c, M. FITTA^d, M. MIHALIK JR.^a,
J. LAZÚROVÁ^a, M. VAVRA^{a,b}

^aInstitute of Experimental Physics SAS, Watsonova 47, 040 01 Košice, Slovakia

^bInstitute of Chemistry, Faculty of Science, P.J. Šafarik University, Moyzesova 11, 041 54 Košice, Slovakia

^cInstitute of Geotechnics SAS, Watsonova 45, 040 01 Košice, Slovakia

^dInstitute of Nuclear Physics, Polish Academy of Sciences, Radzikowskiego 152, Kraków, Poland

Magnetic properties of $\text{La}_{0.8}\text{K}_{0.2}\text{MnO}_3$ have been studied on nanoparticles prepared by glycine-nitrate method. Crystal structure and particles size were modified by heat treatment. Crystal structure changes from orthorhombic (space group $Pbma$) to rhombohedral (space group $R-3c$) after annealing at 600 °C/2 hours. The average size of particle varies with annealing from about 30 nm to 135 nm. The Curie temperature T_C and the saturated magnetization μ_s increase with annealing. The exchange bias effect was observed on samples with particles size smaller than 60 nm.

DOI: [10.12693/APhysPolA.126.312](https://doi.org/10.12693/APhysPolA.126.312)

PACS: 75.50.-y, 75.47.Lx, 75.30.-m, 75.30.Kz

The mixed-valence manganese oxides of the general formula $\text{La}_{1-x}\text{A}_x\text{MnO}_3$ (A is a divalent ion like Ca, Sr, Ba and Pb) are a subject of interest due to a desire to understand and exploit the large negative magnetoresistance and magnetocaloric effects [1]. Among manganites, the manganites doped with univalent metals, such as Ag, K, and Na are of greatest interest, because their physical properties are very sensitive to magnetic field at room temperature. Group of $\text{La}_{1-x}\text{K}_x\text{MnO}_3$ manganites provides a series of new oxides to study magnetocaloric effect [2, 3] and insulator-to-metal transition [4] at room temperature. In our paper we study the effect of annealing on magnetic properties of $\text{La}_{0.8}\text{K}_{0.2}\text{MnO}_3$ nanoparticles.

The preparation of nanoparticles followed the glycine-nitrate method, where glycine was used as a fuel and nitrates as oxidants [5]. The as prepared samples were annealed for 2 hours in air atmosphere at 300 °C, 600 °C and 900 °C.

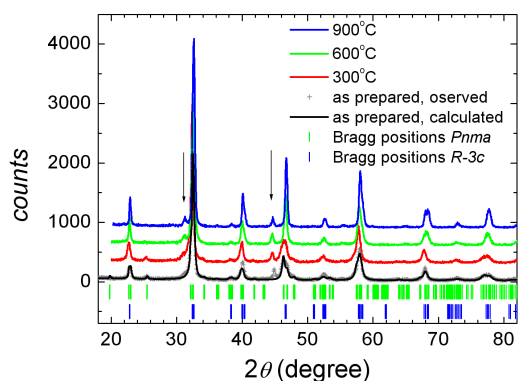


Fig. 1. X-ray powder diffraction patterns for all samples; arrows point to the contribution from sample holder.

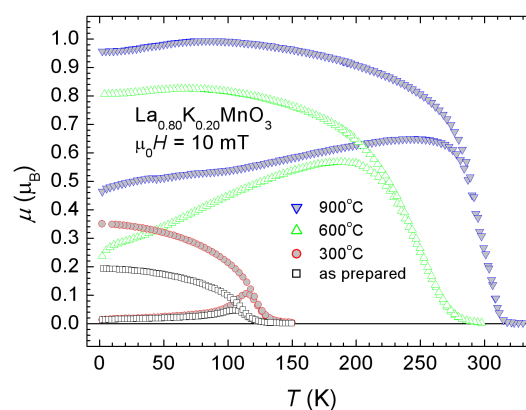


Fig. 2. Magnetization measurements in ZFC and FC regimes for all samples.

The X-ray powder diffraction (XRD) measurements have been carried out on the X'Pert PRO diffractometer with $\text{Cu-K}\alpha$ radiation ($\lambda_1 = 1.54056 \text{ \AA}$, $\lambda_2 = 1.54440 \text{ \AA}$) and the XRD patterns were evaluated with the FullProf program based on the Rietveld method [6]. The as prepared sample and sample annealed at 300 °C adopt orthorhombic crystal structure (space group $Pnma$) with lattice parameters $a = 0.5570(5) \text{ nm}$; $b = 0.7773(9) \text{ nm}$; $c = 0.5525(1) \text{ nm}$. The crystal structure changes to rhombohedral (space group $R-3c$) with annealing, $a = 0.5512(6) \text{ nm}$; $c = 1.3385(2) \text{ nm}$ for the sample annealed at 900 °C. MnO_6 – the building blocks of the crystal structures are distorted and tilted. The average size of nanoparticles depends on annealing and varies between 30 nm and 135 nm. The morphology of nanoparticles and their size distribution was studied on powders by scanning electron microscope (SEM) MIRA3 TESCAN. Magnetization and AC susceptibility measurements were performed by a SQUID (MPMS XL–5) or in a VSM (PPMS) magnetometer in the temperature range from 1.8 K to 380 K and in magnetic field up to 9 T.

Hysteretic behaviour (see Fig. 2) between ZFC and FC magnetization is a characteristic feature of the system.

*corresponding author; e-mail: mihalik@saske.sk

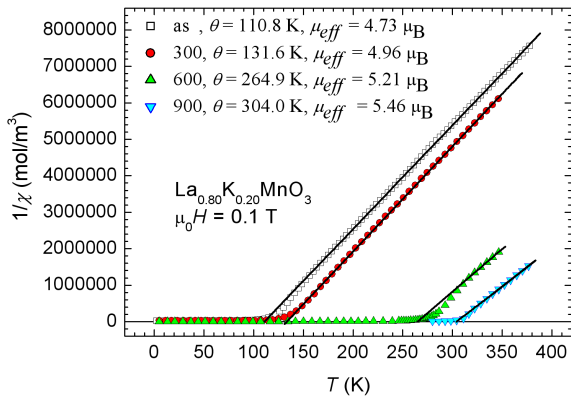


Fig. 3. The inverse susceptibility for all samples, lines represent fits to the Curie-Weiss law.

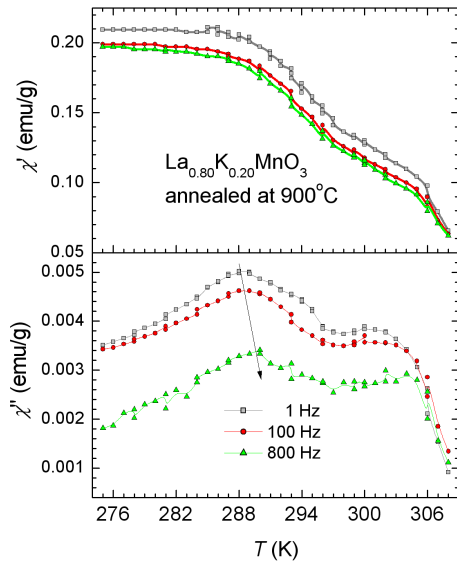


Fig. 4. In phase and out of phase AC susceptibility for the sample annealed at 900 °C.

The increase of ferromagnetic interactions with annealing is evident from all measurements. The Curie temperature increases from $T_C = 112.0$ K to 295.0 K after annealing. The magnetic susceptibility obeys the Curie-Weiss law (Fig. 3) for all samples. The paramagnetic Curie temperature θ and the effective magnetic moment μ_{eff} increase with annealing, indicating the increase of ferromagnetic interactions.

The magnetic phase transition is accompanied with an anomaly in both the real part χ' , and the imaginary part χ'' of AC susceptibility, which are frequency dependent in the case of sample annealed at 900 °C (Fig. 4). In this case two maxima are seen in the susceptibility at the magnetic phase transition (Fig. 4) at $T_{C1} = 288$ K and $T_{C2} = 302$ K, indicating magnetic inhomogeneities in the material. Double transition was observed also in magnetization measurements.

The increase of ferromagnetic correlations in material is seen also from magnetic hysteresis loops measurements.

The saturated magnetization μ_s increases with annealing from $1.54\mu_B$ for sample annealed at 300 °C to $3.29\mu_B$ for sample annealed at 900 °C. The exchange bias effect (EB) was observed on as prepared sample and sample annealed at 300 °C (Fig. 5). In these cases the average particle size is less than 50 nm and core shell model can be applied to explain such behaviour. Cooling down in magnetic field $\mu_0 H_{cf} = 1$ T gives rise to displacement of the magnetic hysteresis loop, which is the typical manifestation of the EB effect. The loop is pinned on vertex in the region of negative magnetization, it is tilted and shifted in horizontal and vertical direction. The horizontal shift of the loop is usually expressed by the exchange bias field $\mu_0 H_E = \mu_0 (H_{c+} - H_{c-})/2 = 1165$ mT; H_{c+} and H_{c-} are the coercive fields on positive and negative axis, respectively. The vertical shift is expressed by the remnant asymmetry $\mu_E = (\mu_{r+} - \mu_{r-})/2 = 0.517\mu_B$; μ_{r+} and μ_{r-} are the remnant magnetizations on the positive or the negative axis, respectively.

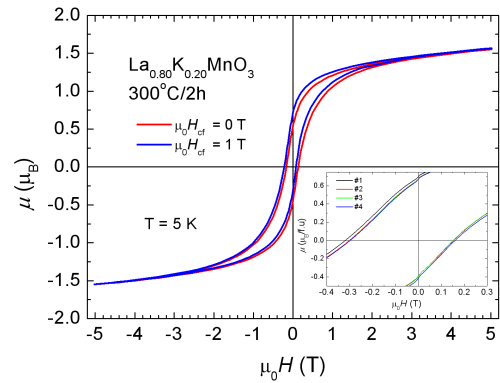


Fig. 5. Exchange bias phenomenon for the sample annealed at 300 °C. The insert shows the training effect after 4 cycles.

This work was supported by the projects VEGA2/0178/13, APVV-0132-11 and ERDF EU under the contract No. ITMS26220120005.

References

- [1] J.M.D. Coey, T. Venkatesan, A.J. Millis, J.R. Cooper, P.C. Riedi, P.B. Littlewood, D.M. Edwards, J.Z. Sun, J. Inoue, *Philosophical Transactions: Math., Phys. and Eng. Sci.* **365**, 1519 (1998).
- [2] A.M. Aliev, A.G. Gamzatov, A.B. Batdalov, A.S. Mankevich, I.E. Korsakov, *Physica B* **406**, 885 (2011).
- [3] I.K. Kamilov, A.G. Gamzatov, A.B. Batdalov, A.S. Mankevich, I.E. Korsakov, *Phys. Solid State* **52**, 789 (2010).
- [4] C. Shivakumara, M.B. Bellakki, *Bull. Mater. Sci.* **32**, 443 (2009).
- [5] D. Markovic, V. Kusigerski, M. Tadic, J. Blanusa, M.V. Antisari, V. Spasojevic, *Scr. Mater.* **59**, 35 (2008).
- [6] M.H. Rietveld, *J. Appl. Cryst.* **2**, 65 (1969).